Development of a Rational Way to Prepare a Highly Active Manganese-Containing Catalyst for Environmentally Friendly Fuel Combustion

S. A. YASHNIK[1], N. V. SHIKINA[1], A. A. GAVRILOVA[1], T. A. SUROVTSOVA[1], Z. R. ISMAGILOV[1,2]

[1]*Boreskov Institute of Catalysis, Siberian Branch, Russian Academy of Sciences,*
Novosibirsk, Russia

E-mail: yashnik@catalysis.ru

[2]*Institute of Coal Chemistry and Material Science, Federal Research Centre of Coal and Coal Chemistry,*
Siberian Branch, Russian Academy of Sciences,
Kemerovo, Russia

Abstract

The temperature-programmed reduction with hydrogen was used to identify the phase composition of the active component and to study redox properties of MnO_x-containing honeycomb monolithic catalysts prepared by two different methods: 1) "solution combustion synthesis" (SCS) on monolith surface; and 2) Co-extrusion of MnO_x powder with oxide components of the monolith. It is assumed that both monolithic catalysts contain predominantly MnO and some amount of MnO_2/Mn_2O_3. Among the studied catalysts, the monolithic catalyst obtained by the SCS method has the maximum activation energy of the second stage of the reduction of MnO_2/Mn_2O_3, which consists in the reduction of Mn_3O_4 to MnO. This explains its high activity in the oxidation of methane.

Key words: manganese-containing catalyst, manganese oxide, MnO_x, TPR-H_2, deep oxidation of hydrocarbon, solution combustion synthesis

INTRODUCTION

Development of the scientific foundations of the rational design of autonomous catalytic heat generators for local heat supply is urgent with respect to fuel saving and the solution of ecological problems of heat-and-power engineering. This problem requires integrated fundamental studies in the area of catalysis, kinetics, fuel combustion and heat engineering. Studies in the area of catalysis and the synthesis of catalysts will allow electing highly active and stable catalysts to provide complete fuel combustion with the minimal emission of hazardous substances [1–4].

To achieve these goals, it is necessary to synthesize the most promising samples of catalysts based on the oxides of transition metals, to study the structural, textural, disperse, morphological and redox characteristics of these catalysts before and after investigations and tests. Catalysts based on manganese oxides are fairly considered to be an alternative to the catalysts containing platinum group metals because of substantially lower prime cost and high activity in the deep oxidation of hydrocarbons and carbon monoxide. Systems based on MnO_x are prone to thermal activation caused by the formation of highly active defect-bearing spinel Mn_3O_4 [5, 6], and to synergism in the oxidative activity in the case if the oxides of transition metals are added [7–9] or insignificant amounts of precious metals [10–13]. Both these effects determine the promising poten-

tial of the use of MnO_x-containing catalysts in catalytic chambers providing ecologically safe fuel combustion in autonomous heating appliances.

The method of catalyst preparation affects its properties including phase composition, morphological, textural, acid and catalytic characteristics. Thus, oxidation-reduction reactions proceeding during thermal treatment form the composition of the catalytically active phase. For instance, thermal decomposition at 550−650 °C causes the transformation of manganese carbonate into Mn_2O_3 in air and into MnO in the inert atmosphere of argon, and the formed MnO is oxidized into Mn_3O_4 even at 400 °C but has low specific surface area [14]. However, even with the same chemical composition of the active phase, the crystal structure (α-, β-, γ-, δ-MnO_2 [15−18]) and morphology (nanotubes, nanorods, nanowire etc. [19]), particle size [20] and the method of MnO_2/Mn_2O_3 bonding on the surface of oxide supports [20] affect the redox properties of MnO_x-containing catalysts prepared from different precursors. Among the known structural modifications of MnO_2 , α- and γ-forms possess the maximal reducing ability [16−18], better chemisorb oxygen [17, 18] and exhibit increased catalytic properties in redox processes, such as the oxidation of CO (β-MnO_2 < γ-MnO_2 < α-MnO_2, δ-MnO_2 [15]) and toluene (β-MnO_2 < δ-MnO_2 < α-MnO_2 < γ-MnO_2 [16]), as well as selective reduction of NO by ammonia [17]. The discussed regularities were established mainly for bulk manganese oxides, while the practical interest for the processes involved in autonomous heat supply and purification of gas emissions from toxic components is focused on the supported catalytic systems based on monolithic ceramic supports.

Among the known methods of the preparation of supported catalysts, the most promising ones are one-stage waste-free methods of the introduction or deposition of MnO_x-containing active component (AC) on a thermally stable support, such as: 1) the incipient wetness impregnation of the ready support (volume of solution = pore volume of the support) with a solution of manganese salt; 2) the introduction of MnO_x powder into the extrusion mass. The possibility of one-stage impregnation to the incipient wetness is limited by the solubility of manganese salts and by the pore volume of the support. In addition, the applicability of the impregnation method may be decreased by the stages of drying and thermal treatment of the catalyst: during these stages, the AC may be carried over to the surface with the formation of nonuniform distribution, the particles of the AC

may get agglomerated, and the phases may be formed through the interaction of the AC with the material of the support. A negative effect of thermal treatment may be decreased by using the so-called solution combustion synthesis (SCS). The method of AC introduction, which involves filling the pores of the support with a solution of manganese salt, makes SCS close to the method of impregnation to the incipient wetness, the only difference being the presence of organic fuel (carbamide, carbohydrazide, hydrazide of maleic acid etc.) in the solution. The listed methods differ by the chemical nature of bonding and the formation of AC particles during the thermal treatment of the catalyst. Within the SCS method, nanocrystalline oxide particles are formed at the moment of the formation of a short-term heat wave [21−24] as a result of a redox reaction between manganese salt and the organic fuel, which decreases the probability of AC particle agglomeration [21] and the interaction with the material of the support. During the thermal treatment of the impregnating catalyst, AC is formed as a result of the thermal decomposition of manganese salt and a solid-phase reaction between MnO_x and aluminosilicate. The outlooks of SCS for the preparation of low-percent catalysts on the monolithic supports of honeycomb structure [25−27] and non-porous structured supports [28, 29] were demonstrated only in a few works. The deposition of the high AC concentrations may cause a decrease in dispersion, which is connected with the limited pore volume and amount of adsorption centres on the surface of the support.

The method of the joint formation of AC powder and the support material allows introducing high concentrations of catalytically active components, though the ready catalyst often contains AC particles decorated with the inert material. The principle of the method relies on the preparation of plastic paste based on AC powders, support material and a binding sol, subsequent extrusion of the paste through a die, crying and thermal treatment. The methods of regulating the texture and mechanical properties of monolithic materials are rather well developed [30, 31]. The size of AC particles and their size distribution may be governed by choosing methods and conditions for the synthesis of catalytically active oxides.

The goal of the present work was to study the regularities of the formation of redox properties of catalysts based on manganese oxides introduced using two methods: 1) SCS; 2) the joint molding of the support material and MnO_x powder synthesized by means of SCS.

EXPERIMENTAL

Catalyst preparation

To prepare catalyst 1, at first, a monolithic support was prepared using extrusion of the plastic paste through a die and subsequent drying at the room temperature for 24 h and at 120 °C for 5 h, followed by annealing at T_{an} = 750 °C for 4 h. The plastic paste was prepared in a Z-shaped mixer by mixing γ-Al_2O_3 and α-Al_2O_3, hydrated clay (humidity 70 %), calcium carbonate and talc at the mass ratio of the components 8 : 25 : 15 : 1.5 : 1, respectively.

The synthesis of catalyst 1 was carried out by means of SCS. This method includes impregnation of the preliminarily prepared monolithic support in the excess of the solution of manganese nitrate $Mn(NO_3)_2$ with the addition of glycine at the molar ratio of Mn/glycine = 1 : 5 and subsequent removal of the excess solution from the channels. Then the sample was dried in the flow of hot air and annealed at a temperature of 550 °C in the air. The concentration of manganese salt in the impregnating solution was calculated for the deposition of 5 mass % MnO_2 and pore volume of the support 0.09 cm^3/g (to achieve the incipient wetness).

Catalyst 2 was prepared by means of extrusion which involved the addition of 0.5 g MnO_x into the plastic paste (10.1 g taking into account the humidity) composed of γ-Al_2O_3 and α-Al_2O_3, hydrated clay (humidity 70 %), calcium carbonate and talc, mixing with a Z-shaped mixer, and extrusion through a die. The ratio of the components of the support in the paste is similar to their ratio in the support used to synthesize catalyst 1. Thermal treatment included drying at the room temperature for 24 h, at 120 °C for 5 h, and annealing at 550 or 750 °C for 4 h. The MnO_x powder was obtained by means of SCS from the concentrated aqueous solution containing $Mn(NO_3)_2$ and glycine (Mn/glycine = 1 : 5) by drying and annealing at 550 or 750 °C for 4 h. The content of MnO_x in the annealed catalyst was 5 mass % calculated for MnO_2.

Catalysts 1 and 2 are designated as MnO_2(gl)/AlSi-550 and MnO_2(gl)-AlSi-550/750, respectively.

Physicochemical properties of the catalysts

The texture characteristics of the support and the catalysts (specific surface area S_{BET} and pore volume V_{por}) were studied by means of the low-temperature desorption of nitrogen in the ASAP 2400 Micro-metrics set-up at 77 K.

X-ray phase analysis (XRA) of the samples was carried out with the help of HZG-4C diffractometer (Freiberger Prazisionsmechanik, Germany) with monochromatic cobalt radiation CoK_{α} (λ = 1.79021 Å) within the angle range 20−80° over 2θ with the scanning rate of 1 deg/min. The samples were identified using the X-ray database JCPDS.

The catalytic activity of the samples was measured in the deep oxidation of methane in a flow reactor made of quartz at a temperature of 200 to 700 °C. We used 1 cm^3 of the catalyst in the form of the fraction with particle size 0.5−1 mm. The initial reaction mixture containing 1 vol. % CH_4 in the air was supplied to the reactor with the gas hour space velocity of 12 000 h^{-1}. Catalytic activity was evaluated from the temperature of 50 % conversion of methane.

Procedure of the TPR-H_2 experiment

Experiments on temperature-programmed reduction by hydrogen (TPR-H_2) were carried out in a set-up equipped with a flow reactor and a thermal conductivity detector. The reduction was carried out within temperature range 25−950 °C, with the rate of temperature rise equal to 10 °C/min passing a mixture of 10 % H_2 in Ar at a rate of 30 cm^3/min through the weighted portion of the sample. Before the experiment, the sample was pretreated in argon flow blown through the reactor at a rate of 30 cm^3/min, at 450 °C for 30 min. The weighted portion of the sample was 100 mg, grain size 250−500 μm. To eliminate exothermal effects, the sample was mixed with 100 mg of quartz with a similar grain size. Water formed in TPR-H_2 was removed from the gas mixture by freezing in a trap at a temperature of −70 °C. Quantitative measurements were carried out with respect to hydrogen consumed for the reduction of CuO under similar conditions assuming that CuO is reduced completely in one stage.

Linearization of the experimental data obtained by means of TPR-H_2, recorded at the heating rates of 5, 10, 15 °C/min, we calculated activation energy (E_a) of MnO_x reduction by hydrogen for some samples using the method proposed by Kissinger [32]:

$$2 \ln T_m - \ln \beta = E_a/(RT_m + C)$$

Here β is heating rate; T_m are temperatures of the maxima of peaks in the TPR-H_2 profile recorded at the given heating rate; R is universal gas constant (8.31 kJ/mol); C is a constant.

RESULTS AND DISCUSSION

Some physicochemical characteristics of the samples are listed in Table 1. Analysis of these data shows that the specific surface area and pore volume of the impregnating and molded catalysts are comparable with each other (29–30 m^2/g and 0.080–0.082 cm^3/g), and with the characteristics of the support (28 m^2/g and 0.086 cm^3/g). The phase composition of monolithic catalysts annealed at the same temperature (550 °C) is identical to the composition of the support: α-SiO$_2$ (quartz) and α-Al$_2$O$_3$ (corundum). The composition of MnO$_x$ was not identified from the XRA data due to its low content in the catalyst, while the major phase of the bulk sample was Mn$_2$O$_3$. The use of TPR-H$_2$ allowed us to assume the phase composition of manganese oxides in monolithic catalysts and at the same time to evaluate their redox properties.

The TPR-H$_2$ profiles of the bulk samples of manganese oxide obtained by means of SCS, with different annealing temperatures 550 and 750 °C, are shown in Fig. 1. A bulk sample of MnO$_x$ annealed at both temperatures is reduced in two stages, and temperature rise leads to the shift of the maxima of hydrogen consumption to the high-temperature region: from 290 to 345 °C (the first maximum) and from 430 to 465 °C (the second maximum). The ratio of the areas of the 1st and the 2nd peaks of hydrogen consumption, as well as total hydrogen consumption, are almost independent of temperature. The ratio H$_2$/Mn was within the range 0.52–0.57, pointing to the presence of Mn$_2$O$_3$ as the major phase-determining oxide. The shift of peak maxima observed with an increase in sample annealing temperature is due to a decrease in the dispersion of Mn$_2$O$_3$ particles.
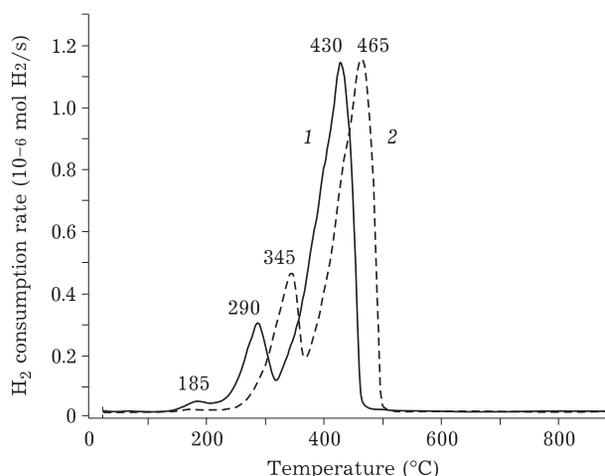
Fig. 1. TPR-H$_2$ profiles for a massive MnO$_x$ sample obtained by SCS mode and differing by calcination temperature, °C: 550 (*1*), 750 (*2*); molar ratio of the amount of consumed hydrogen to the amount of manganese oxide H$_2$/Mn: 0.52 (*1*) and 0.57 (*2*).

In addition, the curve of reduction of a bulk MnO$_x$ sample after annealing at 550 °C contains a peak in the region of 185 °C, which is likely to be due to an insignificant amount of MnO$_2$ in the sample or Mn^{4+} cations on the surface of Mn$_2$O$_3$ particles. An admixture of MnO$_2$ is completely removed after MnO$_x$ annealing at 750 °C, which is quite natural because of the completion of MnO$_2$ decomposition to form Mn$_2$O$_3$ at temperatures above 700 °C [14]. The observed temperature maxima of the reduction of bulk MnO$_x$ sample annealed at 550 and at 750 °C are in good agreement with the literature data on the reduction of Mn$_2$O$_3$. Thus, the reduction of bulk Mn$_2$O$_3$ obtained from manganese carbonate at 550 °C in the air proceeds in two stages at 230 and 400 °C, while Mn$_2$O$_3$ obtained by the decomposition of manganese acetate at 400 °C is reduced at somewhat higher temperatures 305 and 420 °C [14].

Table 1

Physicochemical properties of the support and catalysts

Support and catalysts	T_{an}, °C	S_{BET}, m^2/g	V_{por}, cm^3/g	Phase composition[a]	$T_{50\% CH_4}$[b], °C
MnO$_2$(gl)/AlSi-550	550	30	0.082	α-Al$_2$O$_3$, α-SiO$_2$	505
MnO$_2$(gl)-AlSi-550	550	29	0.080	α-Al$_2$O$_3$, α-SiO$_2$, Mn$_2$O$_3$	625
MnO$_2$(gl)-AlSi-750	750	28	0.085	α-Al$_2$O$_3$, α-SiO$_2$, Mn$_2$O$_3$	645
AlSi-550	550	28	0.086	α-Al$_2$O$_3$, α-SiO$_2$	–
AlSi-750	750	27	0.086	α-Al$_2$O$_3$, α-SiO$_2$	–
MnO$_x$-550	550	59	0.250	Mn$_2$O$_3$	695
MnO$_x$-750	750	42	0.210	Mn$_2$O$_3$	715 (39 %)

[a] α-Al$_2$O$_3$ – corundum phase, α-SiO$_2$ – quartz phase.
[b] Dash means that a 50 % conversion of CH$_4$ is not achieved under the chosen conditions.

Oxide α-Mn_2O_3 obtained by annealing manganese hydroxide at 750 °C is reduced at 360 and 450 °C [33]. In all cases, the ratio between the amounts of hydrogen consumed at the first and the second stages of reduction is close to 1 : 2, which corresponds to the stoichiometry of Mn_2O_3 reduction to Mn_3O_4 (H_2/Mn = 0.17) and then Mn_3O_4 to MnO (H_2/Mn = 0.33).

The effect of the oxides of silicon and aluminium present in clay and formed during annealing on the redox properties of MnO_x obtained preliminarily by means of SCS and then introduced into the molded paste is shown in Fig. 2. For catalyst 2, a negative effect of the aluminosilicate component of the paste on the ability of manganese oxide to be reduced by hydrogen is clearly pronounced. Thus, the start of hydrogen consumption shifts to higher temperatures by 35−60 °C, a high-temperature form of hydrogen consumption appears (600−650 °C), and the ratio H_2/Mn decreases almost by a factor of 2 (from 0.52−0.57 to 0.25−0.29). A reason of the decrease may be the hindrance of the access of hydrogen to MnO_x particles decorated with the aluminosilicate component of the catalyst, and difficult-to-oxidize phases that have not got enough time to be reduced during TPR-H_2. The profile of MnO_2(gl)-AlSi-550 reduction has maxima at 325−350, 410, 500 (weak), 655 °C, while MnO_2(gl)-AlSi-750 has the maxima at 350, 430 °C and an asymmetrical maximum at 600 °C. Similarly to the bulk MnO_x

sample, low-temperature peaks correspond to the reduction of Mn_2O_3 particles proceeding in two stages to MnO through Mn_3O_4. Previously similar results were obtained for the supported systems MnO_x/ Al_2O_3 [16, 34] and MnO_x/SiO_2 [34]. High-temperature peaks at 600/655 °C may point to the strong interaction of MnO_x with the oxide components of the support, up to the formation of new compounds between MnO_x and SiO_2 (or Al_2O_3) in the course of thermal treatment of the monolithic catalyst, for example, manganese aluminate or silicate. It was proved that MnO_x particles with the strong interaction with SiO_2 are reduced at 650 °C [20]. As a rule, MnO_x/Al_2O_3 sample [16] is characterized by unresolved peaks of weak intensity in TPR-H_2 within temperature range 200−650 °C, though for our samples the peaks in the TPR-H_2 profile are sufficiently well resolved.

A comparison of the redox properties of the catalysts of the same composition with AC content 5 mass % (calculated for MnO_2) introduced using different methods − joint molding and SCS − is presented in Fig. 3. It is shown that for the catalysts annealed at the same temperature (550 °C) the impregnation sample (catalyst 1) is reduced at lower temperatures than the molded catalyst (catalyst 2). Temperature maxima characterising the reduction of catalyst 1 are shifted to lower temperatures by 60−100 °C in comparison with catalyst 2. Catalyst 1 has the maxima of hydrogen consumption at 370, 550 and 800 °C, while cata-

Fig. 2. TPR-H_2 profiles for catalyst 2 obtained by adding 5 mass % MnO_x into the molded paste; annealing temperature, °C: 550 (*1*), 750 (*2*); for convenient comparison with the data shown in Fig. 1, the rate of hydrogen consumption by molded samples was multiplied by 20 (×20); for comparison, profile (*3*) for support AlSi(750) is shown; the molar ratio of hydrogen consumed to the amount of introduced manganese oxide (calculated amount) H_2/Mn: 0.25 (*1*) and 0.29 (*2*).

Fig. 3. TPR-H_2 profiles of molded (*1*) and impregnating (*2*) catalyst with the same MnO_x content and annealing temperature 550 °C; molar ratio H_2/Mn: 0.25 (*1*) and 0.17 (*2*).
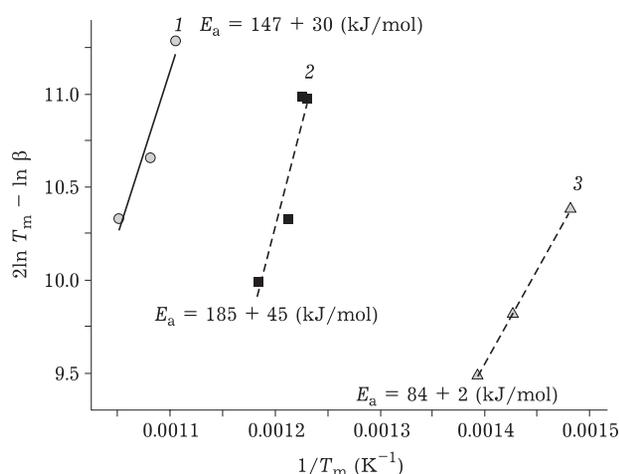
Fig. 4. Activation energy of MnO_x reduction in molded (*1*) and impregnating (*2*) samples of monolithic type, for comparison, the data for bulk MnO_x sample obtained by means of SCS is shown (*3*).

lyst 2 – at 325–350, 410, 500 (weak) and 655 °C. However, the amount of hydrogen consumed during the TPR-H_2 experiment is lower for the impregnating catalyst than for the molded sample (H_2/Mn = 0.17 instead of 0.25, respectively). The latter fact suggests that the major part of AC based on MnO_x is reduced to MnO during its deposition by means of SCS, and the remaining part of MnO_x is incorporated in the composition of the fine MnO_2/Mn_2O_3.

So, both methods of catalyst preparation – 1) deposition of MnO_x by means of SCS, and 2) joint molding of MnO_x with the components of the support – hinder the reduction of MnO_x in comparison with the bulk sample. To study the nature of the interaction of MnO_x with the oxide components of the support, TPR-H_2 experiments with the variation of heating rate were carried out. Through linearization of experimental data (Fig. 4), activation energies (E_a) of the second stage of Mn_2O_3 reduction corresponding to the reduction of Mn_3O_4 into MnO were determined (the second temperature maximum in TPR-H_2 profiles, see Fig. 1–3). Results of these calculations showed that the minimal E_a of Mn_3O_4 reduction into MnO is that exhibited by the bulk sample (84±2 kJ/mol). The joint molding of bulk MnO_x with the oxide components of the support leads to a 1.75-fold increase in E_a (to 147±30 kJ/mol). Among monolithic catalysts, sample 1 obtained with the help of SCS is characterized by the maximal E_a, which is equal to 185±45 kJ/mol. In both cases, an increase in E_a is connected with the interaction between MnO_x and oxide components of the support, which brings the hindrance to the reduction of Mn_3O_4 to MnO.

As discussed above, the stability of Mn_3O_4 under reducing conditions increases in the sequence: bulk sample < catalyst 2 < catalyst 1. It turned out that the temperature of 50 % conversion of methane decreases as the same sequence (see Table 1) and therefore the catalytic activity of the catalysts in the reaction of methane oxidation increases. This trend is quite natural due to the high reactivity of Mn_3O_4 [5, 6] compared to other oxides MnO_x.

CONCLUSION

Preparation of MnO_x-containing monolithic catalysts using two different methods: 1) SCS on the surface of the monolithic support, and 2) joint molding of MnO_x powder (obtained by means of SCS) with the oxide components of the support allows governing the redox properties of the catalyst and therefore its catalytic activity in hydrocarbon oxidation.

According to the data obtained in TPR-H_2 experiments, it is assumed that the phase composition of MnO_x in monolithic catalysts is only weakly dependent on the preparation method, both monolithic catalysts contain mainly MnO and some amount of MnO_2/Mn_2O_3. The major reason for the effects observed during TPR-H_2 and in catalytic experiments is the interaction of MnO_x with the oxide components of the support. In comparison with the bulk sample, this interaction causes a shift of the maxima of hydrogen consumption to higher temperatures, a decrease in the H_2/Mn ratio and increase in E_a of the second stage of the reduction of MnO_2/Mn_2O_3, which involves the reduction of Mn_3O_4 to MnO.

Among the studied samples, the monolithic catalyst obtained by means of SCS on the surface of the ready support possesses the maximal value of the E_a of Mn_3O_4 reduction to MnO and the highest catalytic activity in methane oxidation.

Acknowledgements

REFERENCES

1 Ismagilov Z. R., Kerzhentsev M. A., *Catal. Rev. Sci. & Eng.*, 1990, Vol. 32, No. 1–2, P. 51–103.
2 Ismagilov Z. R., Kerzhentsev M. A., *Catal. Today*, 1999, Vol. 47, No. 1–4, P. 339–346.

3 Ismagilov Z. R., Shikina N. V., Yashnik S. A., Zagoruyko A. N., Khayrulin S. R., Kerzhentsev M. A., Korotkikh V. N., Parmon V. N., Braynin B. I., Zakharov V. M., Favorskiy O. N., *Kinetika I Kataliz*, 2008, Vol. 49, No. 6, P. 922−935.

4 Yashnik S. A., Shikina N. V., Ismagilov Z. R., Zagoruiko A. N., Kerzhentsev M. A., Parmon V. N., Zakharov V. M., Braynin B. I., Favorski O. N., Gumerov A. M., *Catal. Today*, 2009, Vol. 147, P. S237−S243.

5 Tsyrulnikov P. G., Salnikov V. S., Drozdov V. A., Stuken S. A., Bubnov A. V., Grigorov E. I., Kalinkin A. V., Zaykovskiy V. I., *Kinetika I Kataliz*, 1991, Vol. 32 (2), P. 439−446.

6 Tsyrulnikov P. G., Tsybulya S. V., Kryukova G. N., Boronin A. I., Koscheev S. V., Starostina T. G., Bubnov A. V., Kudrya E. N., *J. Molec. Catal. A*, 2002, Vol. 179, P. 213−220.

7 El-Shobaky G. A., El-Shobaky H. G., Badawy A. A. A., Fahmy Y. M., *Appl. Catal. A*, 2011, Vol. 409−410, P. 234−238.

8 Lu H., Kong X., Huang H., Zhou Y., Chen Y., *J. Environ. Sci.*, 2015, Vol. 32, P. 102−107.

9 Shikina N. V., Yashnik S. A., Gavrilova A. A., Doblitova L. S., Khayrulin S. R., Kozlova G. S., Ismagilov Z. R., *Kinetika I Kataliz*, 2018, Vol. 59, No. 4, P. 517−528.

10 Yashnik S. A., Ismagilov Z. R., *Top. Catal.*, 2012, Vol. 55, No. 11−13, P. 818−836.

11 Yashnik S. A., Ismagilov Z. R., Denisov S. P., Danchenko N. M., *Appl. Catal. B.*, 2016, Vol. 185, P. 322−336.

12 Yashnik S. A., Surovtseva T. A., Ischenko A. V., Kaichev V. V., Ismagilov Z. R., *Kinetica I Kataliz*, 2016, Vol. 57, No. 4, P. 535−547.

13 Yashnik S. A., Chesalov Yu. A., Ishchenko A. V., Kaichev V. V., Ismagilov. Z. R., *Appl. Catal. B,* 2017, Vol. 204, P. 89−106.

14 Kapteljn F., Smgoredjo L., Andreml A., Moljin J.A., *Appl. Catal. B*, 1994, Vol. 3, P.173−189.

15 Liang S., Teng F., Bulgan G., Zong R., Zhu Y., *J. Phys. Chem. C*, 2008, Vol. 112, P. 5307−5315.

16 Si W., Wang Y., Peng Y., Li X., Li K., Li J., *Chem. Commun.*, 2015, Vol. 51, P. 14977−14980.

17 Gong P. J., Xie J. L., Fang D., Han D., He F., Li F. X., Qi K., *Chin. J. Catal.*, 2017, Vol. 38, P. 1925−1934.

18 Huang N., Qu Z., Dong C., Qin Y., Duan X., *Appl. Catal. A*, 2018, Vol. 560, P. 195−205.

19 Wang F., Dai H., Deng J., Bai G., Ji K., Liu Y., *Environ. Sci. Technol.*, 2012, Vol. 46, P. 4034−4041.

20 Kapteijn F., van Langeveld A. D., Moulijn J. A., Andreini A., Vuurman M. A., Turek A. M., Jehng J. M., Wachs I. E., *J. Catal.*, 1994, Vol. 150, P. 94−104.

21 Mukasyan A. S., Dinka P., *Intern. J. Self-Propagating High-Temperature Synthesis*, 2007, Vol. 16 (1), P. 23−35.

22 Patil K. C., Hedge M. S., Rattan R., Aruna S. T., Nanocrystalline Oxide Materials. Combustion Synthesis, Properties and Applications, London, World Scientific, 2008.

23 Gonzalez-Cortes S. L., Xiao T.-C., Green M. L. H., *Stud. Sur. Sci. Catal.*, 2006, Vol. 162, P. 817−824.

24 Gonzalez-Cortes S. L., Imbert F. E., *Appl. Catal. A*, 2013, Vol. 452, P. 117−131.

25 Sharma S., Hegde M. S., *Catal. Lett.*, 2006, Vol. 112, P. 69−75.

26 Russo N., Mescia D., Fino D., Saracco G., Specchia V., *Ind. Eng. Chem. Res.*, 2007, Vol. 46, P. 4226−4231.

27 Zavyalova U. F., Barbashova P. S., Lermontov A. S., Shitova N. B., Tretyakov V. F., Burdeynaya T. N., Lunin V. V., Drozdov V. A., Yashnik S. A., Ismagilov Z. R., Tsyrulnikov P. G., *Kinetika I Kataliz*, 2007, Vol. 48 (1), P. 171−176.

28 Ismagilov Z. R., Mansurov Z. A., Shikina N. V., Yashnik S. A., Aldashukurova G. B., Mironenko A. V., Kuznetsov V. V., Ismagilov I. Z., *Nanoscience and Nanotechnology*, 2013, Vol. 3 (1), P. 1−9.

29 Aldashukurova G. B., Mironenko A. V., Mansurov Z. A., Shikina N. V., Yashnik S. A., Kuznetsov V. V., Ismagilov Z. R., *J. Energy Chemistry*, 2013, Vol. 22, P. 811−818.

30 Yashnik S. A., Ismagilov Z. R., Koptyug I. V., Andrievskaya I. P., Matveev A. A., Moulijn J. A., *Catal. Today*, 2005, Vol. 105, P. 507−515.

31 Yashnik S. A., Andrievskaya I. P., Pashke O. V., Ismagilov Z. R., Mulyayn Ya. A., *Kataliz v Promyshlennosti*, 2007, No. 1, P. 35−46.

32 Kissinger H. E., *Analytical Chem.*, 1957, Vol. 29 (11), P. 1702−1705.

33 Leith I. R., Howden M. G., *Appl. Catal.*, 1988, Vol. 37, P. 75−92.

34 Aboukais A., Abi-Aad E., Taouk B., *Materials Chemistry and Physics*, 2013, Vol. 142, P. 564−571.